The Long Bar in the Milky Way. Corroboration of an old hypothesis

M. López-Corredoira[1], A. Cabrera-Lavers[1,2], T. J. Mahoney[1], P. L. Hammersley[1,2], F. Garzón[1,3], C. González-Fernández[1]

[1] *Instituto de Astrofísica de Canarias. C/.Vía Láctea, s/n, E-38200 La Laguna (S/C de Tenerife), Spain*

[2] *GRANTECAN, S. A., C/.Vía Láctea, s/n, E-38200 La Laguna (S/C de Tenerife), Spain*

[3] *Departamento de Astrofísica, Universidad de La Laguna, S/C de Tenerife, Spain*

martinlc@iac.es

ABSTRACT

Recent GLIMPSE data have further confirmed the hypothesis of the existence of an in-plane long bar different from the bulge of the Milky Way with the same characteristics as emphasized some years ago by our team. In this paper, we present two new analyses that corroborate recent and earlier claims concerning the existence in our Galaxy of a long flat bar with approximate dimensions 7.8 kpc $\times$1.2 kpc $\times$0.2 kpc and a position angle of approximately 43°: 1) star counts with *2MASS* All-Sky Release and *MSX* data, which give an excess in the plane region along $0 < l < 30°$ compared with $-30° < l < 0$, and which cannot be due to the bulge, spiral arms, a ring, or extinction; 2) new data on the distance of the long bar using the red clump method, together with recent observations of our own that are compared with our model, and that are in agreement with the long-bar scenario.

Subject headings: Galaxy: structure – infrared: stars

1. Introduction

Among the different stellar components of our Galaxy are a thin and thick disc, a halo, spiral arms, possibly a stellar ring and the bulge/bar. The bar/bulge components (bulge, or bar, or bulge + bar) are perhaps the most difficult to disentangle from other components because of extinction and our perspective of them due to our position in the Galactic plane (Zhao 2000); they have been the topic of recent controversy concerning their morphology (e.g.

Sevenster et al. 1999; Garzón 1999; Merrifield 2004, and references therein). Our hypothesis in this debate has been that there are indeed two components (Hammersley et al. 2001): a bar which is long and in the plane ($-14^\circ < l < +30^\circ$, $|b| <\approx 1.5^\circ$), and a triaxial bulge, which is short and much wider in latitude (observable at $|l| <\approx 15^\circ$, $|b| <\approx 10^\circ$). Their position angles (angle between the major axis and the solar vector radius) might not be coincident, although the latest measurements give values that do not differ greatly: $43^\circ \pm 7^\circ$ for the long bar (Hammersley et al. 2000; hereafter H00); and $28^\circ \pm \sim 8^\circ$(syst.) for the triaxial bulge (López-Corredoira et al. 2005).

The story of the Galactic bar really begins with the discovery of large non-circular velocities in the 3 kpc and 135 km/s spiral arms (Rougoor & Oort 1960; Rougoor 1964). De Vaucouleurs (1964) was the first to attempt to explain the motions of these arms in terms of a non-axisymmetric potential (a bar) at the centre of the Galaxy. He later predicted that the Milky Way was of type SAB(rs)bc on the grounds of the Galaxy's high spiral arm multiplicity, broken ring structure and non-circular H I motions (de Vaucouleurs 1970). The non-axisymmetry hypothesis, or "field model", was not well received at the time by the astronomical community, which favoured Oort's (1977) "ejection model", advocating the expulsion of gas from the centre of the Galaxy, even though it would require energies of the order 10^{55} erg to power such an expansion of the spiral arms (van der Kruit 1971). Kerr (1967), however, explained the 3 kpc and 135 km/s arms in terms of a bar. Peters (1975) modelled the H I distribution derived from l–v diagrams in the inner 4 kpc of the Galaxy in terms of concentric elliptical orbits. He found that an orientation of 45 deg w.r.t. to the solar radius vector fitted the maximum number of radio features in the l–v diagrams, including the 3 kpc and 135 km/s arms. With regard to molecular gas, Nakai (1992) compared CO ($J = 1 \rightarrow 0$) emission maps of the barred spiral galaxies Maffei 2, NGC 2903 and NGC 253 with that of the Milky Way Galaxy (derived from the CO radial velocity at a sample of galactic longitudes). All four galaxies show a similar radial CO distribution with a sharp central peak and a secondary hump (corresponding to the bar–spiral arm transition). The radio evidence, then, gave strong indications of: a) a non-axisymmetric distribution of gas orbits and b) a CO intensity distribution that corresponded with other barred galaxies.

Our hypothesis concerning the existence of a long bar originate from near-infrared Two Micron Galactic Survey data (TMGS, Garzón et al. 1993). It began with an analysis of K-band TMGS star counts that led Hammersley et al. (1994) to posit the existence of a bar of radius 4 kpc, with one of the tips at $l = 27^\circ$, and the other one at $l = -22^\circ$, which would give an angle of 75 degrees [1]. Calbet et al. (1995) presented "tomographs" of the Galactic plane

[1]This was later retracted by H00, who realized that the negative tip is in fact at $l \approx -12^\circ$, so that the angle of the bar is instead $\approx 43^\circ$.

(derived from TMGS star counts and using the rather inaccurate assumption of a Dirac delta luminosity function, which could serve as a zeroth order approximation of the structure of the Galaxy), and the long bar was evident (figure 14 of Calbet et al. 1995), extending over a radius larger than 3–3.5 kpc, although the method was not accurate enough to provide information about its morphology. Calbet et al. (1996) also proposed the existence of a dust lane preceding the bar at negative longitudes, which would explain the higher extinction observed in this region. Considerable progress was made by H00, who measured the distance of several points along the bar, including $l = 27°$, and, using a technique of analysis of red-clump stars in near-infrared colour–magnitude diagram, concluded that the angle was $43° \pm 7°$. The same analysis with the same data, only using near-infrared filters, was presented by Picaud et al. (2003), who also compared the data with the Besançon model (Robin et al. 2003), and they obtained a similar result ($45° \pm 9°$). Other papers of our team (Garzón et al. 1997; López-Corredoira et al. 1999, 2001b) have produced further evidence, as will be described in Section 2.

Concerning the stellar populations, Ng (1998) finds two populations towards the Galactic Centre: an old metal rich population ($Z = 0.005$–0.08, $t = 13$–15 Gyr), presumably the old Galactic bulge, and a younger less metal-rich population ($Z = 0.003$–0.03, $t = 8$–9 Gyr), perhaps the long bar. Cole & Weinberg (2002) also showed a non-axisymmetric structure that is likely to have been formed more recently than 3 Gyr ago and must be younger than 6 Gyr. However, they are at $|b| > 2°$ so they were possibly measuring the suburbs of the long bar, some anomalously young population in the bulge, or some contamination of the disc.

It is supposed that bars form as the result of an instability in differentially rotating discs (Sellwood 1981) whereas bulges are a primordial galactic component, so this distinction makes sense and it is not merely an artefact invented to fit certain morphological features. Athanassoula & Misiriotis (2002), Athanassoula (2005) and Athanassoula & Beaton (2006) use N-body simulations to produce long bars, which are broadened in at their centres into boxy bulges (the ratio of sizes between the semi-axis of the long bar and the major axis of the boxy bulge is approximately 1.5). Boxy bulges are in fact just a part of the long bar (Athanassoula 2005). From a comparison of their N-body simulations and near-infrared photometry Athanassoula & Beaton (2006) argue that the boxy bulge of M31 extends into a long bar. There is a striking parallel with our own Galaxy, which also has a boxy bulge (Picaud & Robin 2004; López-Corredoira et al. 2005) that extends into the long bar described in this and previous papers. Bars might be vertically extended (Kuijken 1996) but they might be constrained to the plane too. Indeed, many other galaxies exhibit both a bar and a bulge; e.g. NGC 3351, NGC 1433 and NGC 3992, whose images in the Palomar plates, for instance, show the existence of both structures.

Nevertheless, many authors (reviewed by Merrifield 2004) have for many years ignored the bar + bulge hypothesis and preferred to speak about a unique non-axisymmetric structure, namely a bar (i.e. bulge) that is triaxial, short and fatter (what we call this component the bulge). These authors did not consider the possibility of a long bar constrained in the Galactic plane. Although they were more or less successful in fitting the stars in off-plane regions, the abundance of new data now indicates that some new component in the Galactic plane at longitudes $+15^\circ < l < +30^\circ$ is being observed that is unexplainable in terms of a disc + bulge + extinction model. This fact will be corroborated in §2 with All-Sky *2MASS* and *MSX* data. In addition, in §3 we use red clump star data from the recent literature (including new observations of our own: Cabrera-Lavers et al. 2006b) to reinforce the old picture of our hypothesis that there is a long bar apart from the bulge. Furthermore, the position angle obtained in the past is confirmed by the latest data (Benjamin et al. 2005).

2. The asymmetry in the counts

López-Corredoira et al. (2001b) used star counts and extinction maps of negative latitudes and confirmed the general picture of a long bar: higher counts in the positive than in negative longitudes (for $|l| < 30^\circ$ and strictly in the plane $b <\approx 1.5^\circ$). This north/south asymmetry was confirmed with recenter GLIMPSE data by Benjamin et al. (2005), with 25% more sources in the north, although they do not include the region $|l| < 10^\circ$. López-Corredoira et al. (2001b) also show a higher extinction on average iat negative latitudes. Babusiaux & Gilmore (2005) say, however, that they see no asymmetry in the extinction, but we think they have only four points to measure the asymmetry, and one of them ($l \approx -10^\circ$) has a minimum according to López-Corredoira et al. (2001b, Fig. 8). When the star counts are statistically corrected for extinction by using the colours, a clean image of the negative latitudes of the Galaxy is obtained (López-Corredoira et al. 2001b, fig. 10) that clearly shows the in-plane bar extending up to $l \approx -13^\circ$, as expected by H00. The schematic representation in López-Corredoira et al. (2001b, fig. 3) summarizes the model. Unavane & Gilmore (1998) and Alard (2001) also explored asymmetries in star counts in the plane but only for $|l| <\approx 4^\circ$.

With the data of *2MASS* All-Sky data release (Skrutskie et al. 2006) in the K band, we plot the star counts up to $m_K = 9$ in Fig. 1, and show a clear asymmetry. We corroborate the results by López-Corredoira et al. (2001b), who used DENIS and TMGS data for some regions (not all-sky) to claim that a long bar must be present, and that this structure is beyond the bulge region ($|l| < 15^\circ$), extending to nearly $l = 30^\circ$ in positive longitudes.

With *MSX* mid-infrared data (Egan et al. 1999) we also see the same trend. Figure

3 clearly shows the excess at positive galactic longitudes; it also shows a deficit between $l = -15°$ and $l = -18°$, which indicates that the bar at negative latitudes finishes at $l \approx -14°$ (the feature at $l = -22°$ is thought to be the 3 kpc ring; López-Corredoira et al. 2001b).

Garzón et al. (1997) and López-Corredoira et al. (1999) confirmed spectroscopically that most of the brightest K-band stars at $l = 27°$ in the plane are supergiants, thereby reinforcing the argument that this region contains a prominent star formation region possibly associated with the end of the bar where it meets the Scutum spiral arm.

Freundenreich (1998) realized that there are significant residuals in the plane over $|l| < 30°$ after subtracting the disc and the bulge in *COBE*/DIRBE data; however, he prefers to attribute these residuals to patchy star formation in a ring or spiral arms. Picaud (2004) also says that this star formation region might be associated with some other structure such as a ring. However, as plotted in López-Corredoira et al. (2001b, fig. 6), a ring would produce a shape in the distribution of star counts different from that shown in Figure 1. Moreover, the deficit of stars observed between $l = -15°$ and $l = -18°$ in Fig. 3 indicates the absence of any possible continuous structure between $l = 0$ and $l = -22°$; a ring should be continous, whereas our bar finishes at $l = -14°$. The bar fits the star counts perfectly, whereas the ring does not. A spiral arm solution on the far side of the Galaxy (at distance 10–12 kpc) or closer than the central region of the Galaxy (distances less than 5 kpc) is also discarded because of the arguments given by Hammersley et al. (1994) and because, as will be shown in §3, the distance of this structure does not fit any ring or spiral arm possibility.

Extinction is also discarded by Hammersley et al. (1994) and López-Corredoira et al. (2001b). Furthermore, a closer examination of extinction-corrected counts, for instance that in López-Corredoira (2005, fig. 1), shows a still higher number of counts at positive longitudes. In Fig. 2 we show an example from the data of López-Corredoira et al. (2005) with $m_e < 7.0$. GLIMPSE (Benjamin et al. 2005) and *MSX* mid-infrared data (Fig. 3) also show the asymmetry and are much less affected by extinction.

3. The red clump as a distance indicator

The red clump method is well known and explained in several papers (e.g. Stanek et al. 1997; H00; López-Corredoira et al. 2002): in a colour–magnitude diagram, the maximum of the density of the red clump stars is identified with the major axis of the bar along each line of sight. This is not strictly true; it is a good approximation only when the bar is thin,

that is, a very elongated structure, a long bar rather than a thick bulge. In our case, the bar is thin because there is a dispersion of $\sigma \approx 0.5$–0.6 mag for the red clump, including the intrinsic broadening of the red clump itself and the dispersion of distances (Fig. 4). In a thick bulge, the maximum density in the line of sight is at the tangential point of the line of sight with the ellipsoids and may differ from the major axis position by $\sim$1 kpc, but the difference is only $\sim$50 pc for the thin bar (appendix A). Also, there is a difference between the maximum density along the line of sight and the maximum of the star counts of the red clump vs. the apparent magnitude, which is again negligible for thin bars (25–50 pc) and somewhat more important for the thick bulge (100–300 pc) (appendix B). Some authors, e.g. Babusiaux & Gilmore (2005), have not considered these effects and applied the method to fit the major axis of a thick-bulge structure, which is very inaccurate.

By gathering the different data in the literature[2] with measurements of the distance as function of galactic longitude in the Galactic plane (constrained to $|b| <\approx 1^\circ$), we get Fig. 5, which includes data from:

- H00: Datum at $b = 0$, $l = 27^\circ$ at a distance of 5.7 kpc. Other data might perhaps be derived from their colour–magnitude diagrams but, as explained in Cabrera-Lavers et al. (2006b), the crowded regions in the plane limit the validity of the method.

- Picaud et al. (2003). Data at $b = 0$. We take the given distances of 5.9 kpc at $l = 26^\circ$ and $l = 27^\circ$.

- Nishiyama et al. (2005). These authors present many points between $l = -10^\circ$ and $l = +10^\circ$, and we take one for each degree for our plot. Their data are for $b = +1^\circ$, but we assume they are at the same distance as the $b = 0$ data. They also use the red clump method and find that the position angle for $|l| < 4^\circ$ is different from the position angle derived with all the data $|l| < 10^\circ$. They attribute this to the existence of a new structure at $|l| < 4^\circ$ but we believe that this could possibly be the effect of a superposition of a bulge and a long bar. In Fig. 5, we show how their data are roughly compatible with a bar of position angle 40–45 degrees.

- Babusiaux & Gilmore (2005). Data at $b = 0$ (except the point at $l = 0$, which is at $b = +1^\circ$). A value of $R_\odot = 8$ kpc is adopted. Babusiaux & Gilmore (2005) observed in the near infrared with the CIRSI survey in the plane fields at $l = 0$, $\pm 5.7^\circ$, $\pm 9.7^\circ$. They calculate the distance of the red clumps for the bar for each of the five points.

[2]Red clump distance data from Stanek et al. (1997) are not valid for our analysis because they are all more than 2 degrees away from the plane.

Their results are that all the points except $l = -9.7°$ fit a bar with a position angle of 22.5°. The field at $l = -9.7°$ is chosen to contain the presence of a stellar ring or pseudo-ring at the end of the bar. The field at $l = +5.7°$ presents a wide dispersion of distance owing perhaps to the added presence of distant (i.e. at the other side of the bar) disc red clump stars. We think that Babusiaux & Gilmore are observing the long bar and that the angle that their data give is possibly compatible with a position angle of around 40–45 degrees, as is shown in Fig. 5. However, they reject this hypothesis on the grounds that, in their view, a bulge + bar would produce a spread in the red clump distances; possible alternative explanations are that the bar might be predominant in the plane, that the angle of bulge and bar might be very similar in the plane, or that the spread real but low to separate both populations.

- Benjamin et al. (2005). We calculate from their fig. 4, based on GLIMPSE data, the equivalent distances, assuming $R_\odot = 8$ kpc instead of 8.5 kpc (which gives $M_{[4.5]} = -2.02$ instead of -2.15 for the red clump giants), and assuming in this filter 0.05 mag/kpc of extinction. Between $l = +12°$ and $l = +28°$ every four degrees, except $l = 24°$, which is in a high extinction region and no hump associated with the red clump is observed. These GLIMPSE data have recently been analysed by Benjamin et al. (2005), who found that, when plotting the power law exponent of the star counts in the mid infrared (their Fig. 2), a different structure distinct from the disc can be observed for $|l| <\approx 30°$, a hump superimposed on the disc counts. They suggest this to be due to the red clump giants of the long bar. They measured the position angle to be $44 \pm 10°$. Indeed, fig. 1 of Benjamin et al. (2005) also shows quite clearly how the star counts in the mid infrared (with very low extinction) trace an in-plane structure between $l = -14°$ and $l = +30°$. This rediscovery of the long-bar has revived interest in the hypothesis.

- Cabrera-Lavers et al. (2006b). We add new data for b between -1° and +1°, and l between +18° and +28°. The source of the data is the same that of H00 and Picaud et al. (2003) but with more recent observations: TCS-CAIN data (Cabrera-Lavers et al. 2006a).

Figure 5 shows how the data fit the H00 bar with a position angle of $43° \pm 7°$. The error bars of the points represented are roughly 700 pc at 5.7 kpc ($l = 27°$) from the Sun (H00) and somewhat higher for lower values of l; many authors give lower errors for their points but we think they were over-optimistic in their estimation of systematic and random errors. Most of the points are within the expected prediction for the H00 long bar. Perhaps the dispersion of points in the data of Cabrera-Lavers et al. (2006b) indicates that the error in distance is higher than 700 pc. There is one point (at $l = +9.7°$: $x = 887$ pc, $y = 5247$

pc) in Babusiaux & Gilmore (2005) that does not fit the long bar. This point is possibly in error or contaminated by the bulge. The presence of this point is used by Babusiaux & Gilmore (2005) to claim that the bar position angle is 22.5° (a fit made with only 3 points and rejecting the point at $l = -9.7°$), but in view of all the other data, it is more likely that we have to reject instead the point at $l = +9.7°$. Values for the position angle lower than 35 degrees fail to fit all these data.

This angle of around 40–45 degrees also agrees with previous estimates. Peters (1975) modelled the H I distribution with an orientation of 45 deg. The first direct evidence of a large stellar bar was produced by Weinberg (1992), who used AGB stars from the *IRAS* Point Source Catalog (1985) to trace the stellar density distribution within the solar circle. In spite of his simplistic assumptions of a homogeneous AGB sample with a low dispersion in luminosity and dust extinction proportional to distance within the solar circle, Weinberg gave estimates of the bar orientation (36 ± 10 deg) and semilength (∼5 kpc). Sevenster et al. (1999) measured a position angle of 45 degrees when analysing the structure in the plane (and 25 degrees in off-plane regions, which denotes the absence of a bar and only the presence of a triaxial bulge away from the plane). van Loon et al. (2003) detected the long bar at a Galactocentric radius of $R \geq 1$ kpc and measured a position angle, $\phi \sim 40°$. Groenewegen & Blommaert (2005) measured $\phi = 47 \pm 17°$ in the relationship between the zero point of the K-band period–luminosity relation of Mira variables and galactic longitude although they included data between $b = -1.2°$ and $b = -5.8°$ within $|l| < 12°$, so this corresponds to the long bar + thick bulge.

4. Other parameters of the bar

In Table 1 we summarize the parameters of the bar. The major axis semilength, 3.9 kpc, is derived assuming that the end of the bar is at $l = 27°$, that the angle of the bar is 43°, and that the distance to the Galactic Center is $R_\odot = 8$ kpc. The thickness may be derived, as we have said, from the dispersion in the red clump stars, which is roughly 0.5–0.6 mag (H00; Benjamin et al. 2005; Cabrera-Lavers et al. 2006b). In particular, a fit of the data with $|b| \leq 1°$ from Cabrera et al. (2006b) (plotted in Fig. 4) gives:

$$\sigma_{\rm red\ clump} = (0.640 \pm 0.037) - (0.0044 \pm 0.018)\ l(deg.)\ {\rm mag} \quad (1)$$

We assume an intrinsic Gaussian dispersion of the red clump of 0.3 ± 0.1 mag (López-Corredoira et al. 2002) and consider the variation in height along the line of sight of the bar within $|b| \leq 1°$ to be negligible. We also take into account that, because the orientation of

the bar, the angle between the line of sight and the direction perpendicular to the bar is $\alpha = 90^\circ - 43^\circ - l$ (so we must multiply the thickness along the line of sight by a factor $\cos\alpha$) and the distance of the bar is $r(l) = R_\odot \frac{\sin 43^\circ}{\sin(43^\circ + l)}$, so that

$$\sigma_{\text{thickness bar}} \approx (1420 \pm 170) - (12.6 \pm 5.6)\ l(deg.)\ \text{pc}. \quad (2)$$

This would be the horizontal thickness of the bar (within which $\approx 68\%$ of the stars are contained). For low values l it becomes thicker because it is mixed with the bulge. For galactic longitudes around $l \approx 20^\circ$, the thickness is 1170 ± 200 pc. Between $l = 20^\circ$ and $l = 30^\circ$ it is nearly constant.

The vertical thickness is derived when we examine the decrease in the red clump stars in Cabrera-Lavers et al.'s (2006b) data, giving a number of around 200 pc (i.e. a scaleheight of around 100 pc both in the north and in the south).

The mean density is derived by means of

$$\text{Excess counts}(m_K < 9, l) \approx \omega[\Delta r(l)] r(l)^2 \phi[M_K < 9 - 5\log_{10} r(l) + 5 - A_K(r(l), l)]\overline{\rho}.$$

From Fig. 1, the excess counts in positive longitudes over negative longitudes is ≈ 1000 deg^{-2} [surface: $\omega = 1$ deg$^{-2} = 3.0 \times 10^{-4}$ rad^{-2}], roughly independent of l. $\Delta r(l) = \frac{\sigma_{\text{thickness bar}}}{\sin(43^\circ + l)}$. The extinction $A_K(r(l), l) \approx 1.2$ (López-Corredoira et al. 2001b), roughly independent of l. For $l = 20^\circ$, $r(l) = 6.1$ kpc, which gives $M_{K,\max} = 9 - 5\log_{10} r(l) + 5 - A_K(r(l), l) = -6.1$. Hence,

$$\phi[M_K < -6.1]\overline{\rho} = 7 \times 10^{-5}\ \text{star pc}^{-3}, \quad (3)$$

a factor 4 lower value than the rough calculations in López-Corredoira et al. (2001b, §6.2), mainly due to the different thickness used here.

Roughly speaking, if we assume as a model for the bar a box of dimensions $7.8 \times 1.17 \times 0.3 = 2.7$ kpc^3 with average density of stars up to $M_K = -6.1$ equal to $\phi[M_K < -6.1]\overline{\rho}(l = 20^\circ) = 7 \times 10^{-5}$ pc^{-3}, the total number of stars up to absolute magnitude -6.1 is $\sim$200000. For comparison, the bulge up to this absolute magnitude has around 600 000 stars (López-Corredoira et al. 2000, §6.5), so the bar has a third as many stars as the bulge at this range of magnitudes. These bright stars would represent a fraction 2×10^{-5} [from the integration of the bulge luminosity function in López-Corredoira et al. 2000] of the total number of stars; that is, if we assume a similar ratio for the bar, $\overline{\rho} \approx 3.5$ star pc^{-3}.

We cannot derive directly the mass of the bar from the present numbers. We would need a stellar library with an exact knowledge of the population of the long bar, which is a task for a future work. If we assumed roughly that the populations of the thick bulge and the long bar were similar, since the long bar has a third as many bright stars as the thick

bulge and the bulge has 1.7×10^{10} $M_\odot$ (Sevenster et al. 1999), the bar would have $\sim 6 \times 10^9$ $M_\odot$.

Since this article is concerned solely with star counts based on NIR photometry, the kinematics of the bar cannot be discussed here, but other authors have studied it; e.g. Debattista et al. (2002), although these authors do not distinguish between a thick bulge and a long bar. It remains to be studied whether or the thick bulge and the long bar have the same pattern speed. A project dedicated to measuring with accuracy the velocities of the plane stars at $0° < |l| < 30°$ would be warranted. Forthcoming surveys such as *RAVE* (Steinmetz et al. 2006) will in this sense provide valuable information for separating the different components along the line of sight in the central plane regions.

5. Bulge contamination

Throughout the present paper we have presented two kinds of data that show the presence of the bar: 1) counts of bright stars and 2) results from the red clump method. In both cases, the presence of the bulge is important only for low values of galactic longitude:

1. The star counts in Fig. 2 give an excess of ∼1000 stars deg^{-2} in positive galactic longitudes. According to the models in López-Corredoira et al. (2005; Model 1), the contribution of the thick bulge in the plane for these magnitudes is lower than 20% of this amount for $l < -9.5°$ or $l > 13°$ and lower than 10% of this amount for $l < -12°$ or $l > 17°$. This can indeed be observed in the Fig. 2, where the decreasing density of the bulge is not significant away from $|l|$ equal to 10 or 12 degrees. Therefore, the (nearly flat) excess of counts for higher $|l|$ values than these make no significant contribution to the bulge. The same applies to Fig. 1 and the *MSX* bar counts of Fig. 3 (to be

Table 1: Approximate parameters of the long bar

Parameter	Value
Angle Galactic Center–major axis:	43°
Major semiaxis length:	3900 pc
Horizontal thickness at $l = 20°$:	1170 pc
Vertical thickness at $l = 20°$:	200 pc
Star density at $l = 20°$, $b = 0$ with $M_K < -6.1$:	7×10^{-5} pc^{-3}
Total mass (assuming bulge stellar pop.):	6×10^9 $M_\odot$

compared with the bulge counts in López-Corredoira et al. 2001a).

2. The density of red clump stars is proportional to the total density of stars. The bulge along the major axis of the bar has a density $6.6 \exp[-1.1 x_1/(740\ \mathrm{pc})]$ star pc^{-3} (López-Corredoira et al. 2005), where x_1 is the distance from the center. If we take the value of the star density in the bar estimated in §4 as a $\overline{\rho} = 3.5$ star pc^{-3}, the bulge would be responsible for 20% of the bar counts at $t = 1510$ pc (equivalent to $l = 8.5°$) and 10% of the bar counts at $t = 1970$ pc (equivalent to $l = 11.5°$). For longitudes lower than 8.5° ($|x| < 1000$ pc in Fig. 5) the bulge contaminates more than 20% of the bar contribution so we are measuring the position angle of a mixture of two populations.

6. Conclusions

Our conclusion is therefore that recent available data on the long bar corroborate H00's hypothesis. The Milky Way has a long thin bar with approximate dimensions 7.8 kpc ×1.2 kpc ×0.2 kpc; a position angle of the major axis with respect to the line Galactic center-Sun of approximately 43°; density of stars (brighter in K-band than $M_K = -6.1$) around 7×10^{-5} pc^{-3}, and approximately the third part of stars of the thick bulge if we assume similar stellar populations for both components. GLIMPSE data (Benjamin et al. 2005) explicitly supported this model, and other data on the distance of the long bar derived with the red clump method agree in general with this scenario.

Acknowledgments

M. López-Corredoira was supported by the *Ramón y Cajal* Programme of the Spanish Science Ministry. This publication makes use of data products from the Two Micron All Sky Survey, which is a joint project of the University of Massachusetts and the Infrared Processing and Analysis Center/California Institute of Technology, funded by the National Aeronautics and Space Administration and the National Science Foundation. The MSX Point Source Catalog was obtained from the NASA/IPAC Infrared Science Archive at Pasadena, California.

REFERENCES

Alard, C. 2001, A&A 379, L44

Athanassoula, E., 2005, MNRAS, 358, 1477

Athanassoula, E., & Beaton, R. L., 2006, MNRAS, 370, 1499

Athanassoula, E., & Misiriotis, A., 2002, MNRAS, 330, 35

Babusiaux, C., & Gilmore, G. 2005, MNRAS 358, 1309

Benjamin, R. A., Churchwell, E., Babler, B. L., et al. 2005, ApJ 630, L149

Cabrera-Lavers, A., Garzón, F., Hammersley, P. L., Vicente, B., & González-Fernández, C., 2006a, A&A, 453, 371

Cabrera-Lavers, A., et al. 2006b, A&A, submitted

Calbet, X., Mahoney, T., Garzon, F., & Hammersley, P. L. 1995, MNRAS 276, 301

Calbet, X., Mahoney, T. J., Hammersley, P. L., Garzón, F., & López-Corredoira, M. 1996, ApJ, 457, L27

Cole, A. A., & Weinberg, M. D. 2002, ApJ 574, L43

de Vaucouleurs, G., 1964, in: The Galaxy and the Magellanic Clouds, ed. F. Kerr & A. Rodgers (Canberra: Australian Acad. Sci.), p. 195

de Vaucouleurs, G. 1970, in: The Spiral Structure of our Galaxy, ed. W. Becker & G. Contopoulos (Dordrecht: Reidel), p. 18

Debattista, V. P., Gerhard, O. E., & Sevenster, M. N. 2002, MNRAS, 334, 355

Egan, M. P., Price, S. D., Moshir, M. M., Cohen, M., & Tedesco, E. 1999, The Midcourse Space Experiment Point Source Catalog Version 1.2 Explanatory Guide, Air Force Research Laboratory Technical Report, AFRL-VSTR 1999-1522

Garzón, F., 1999, in: The Evolution of Galaxies on Cosmological Timescales (ASP Conf. Ser. 187), J. E. Beckman, T. J. Mahoney, Eds., ASP, S. Francisco, p. 31

Garzón, F., Hammersley, P. L., Mahoney, T., Calbet, X., Selby, M. J., & Hepburn, I. D. 1993, MNRAS, 264, 773

Garzón, F., López-Corredoira, M., Hammersley, P. L., Mahoney, T. J., Calbet, X., & Beckman, J. E. 1997, ApJ 491, L31

Groenewegen, M. A. T., & Blommaert, J. A. D. L. 2005, A&A 443, 143

Freundenreich, H. T. 1998, ApJ, 492, 495

Hammersley, P. L., Garzón, F., Mahoney, T. J., & Calbet, X. 1994, MNRAS, 269, 753

Hammersley, P. L., Garzón, F., Mahoney, T. J., López-Corredoira, M., & Torres, M. A. P. 2000, MNRAS 317, L45 (H00)

Hammersley, P. L, López-Corredoira, M., & Garzón, F., 2001, in: Tetons 4: Galactic Structure, Stars and the Interstellar Medium, ASP Conf. Ser. 231, C. E. Woodward, M. D. Bicay, J. M. Shull, eds., ASP, S. Francisco, p. 81

Kerr, F. J. 1967, in: Radio Astronomy and the Galactic System (IAU Symp. 31) H. van Woerden, ed, Academic Press, London, p. 239

Kuijken K. 1996, in: Unsolved problems of the Milky Way (IAU Colloq. 169), eds. L. Blitz, & P. Teuben, Kluwer, Dordrecht, p. 71

López-Corredoira, M., Garzón, F., Beckman, J. E., Mahoney, T. J., Hammersley, P. L., & Calbet, X. 1999, AJ, 118, 381

López-Corredoira, M., Hammersley, P. L., Garzón, F., Simonneau, E., & Mahoney, T. J. 2000, MNRAS, 313, 392

López-Corredoira, M., Cohen, M., & Hammersley, P. L. 2001a, A&A, 367, 106

López-Corredoira, M., Hammersley, P. L., Garzón, F., Cabrera-Lavers, A., Castro-Rodríguez, N., Schultheis, M., & Mahoney, T. J. 2001b, A&A 373, 139

López-Corredoira, M., Cabrera-Lavers, A., Garzón, F., & Hammersley, P. L. 2002, A&A, 394, 883

López-Corredoira, M., Cabrera-Lavers, A., & Gerhard, O. E. 2005, A&A, 439, 107

Merrifield, M. R. 2004, in: Milky Way Surveys: The Structure and Evolution of our Galaxy (ASP Conf. 317), D. Clemens, R. Shah, & T. Brainerd, eds. Astronomical Society of the Pacific, S. Francisco, p. 289

Nakai, N. 1992, PASJ, 44, L27

Ng Y. K. 1998, in: The Central Regions of the Galaxy and Galaxies, IAU Symp. 184, Y. Sofue, ed., Kluwer, Dordrecht, p. 27

Nishiyama, S., Nagata, T., Baba, D., et al. 2005, ApJ 621, L105

Oort, J. H. 1977, ARA&A, 15, 295

Peters III, W. L. 1975, ApJ, 195, 617

Picaud, S., 2004, in: Milky Way Surveys: The Structure and Evolution of our Galaxy (ASP Conf. 317), D. Clemens, R. Shah, & T. Brainerd, eds. Astronomical Society of the Pacific, S. Francisco, p. 142

Picaud, S., Cabrera-Lavers A., & Garzón F. 2003, A&A 408, 141

Picaud, S., & Robin, A. C. 2004, A&A, 428, 891

Robin, A. C., Reylé, C., Derrière, S., & Picaud, S. 2003, A&A, 409, 523

Rougoor, G. 1964, Bull. Astron. Inst. Netherlands, 17, 381

Rougoor, G. & Oort, J. H. 1960, Proc. Nat. Acad. Sci., 46, 1

Sellwood J. 1981, A&A 99, 362

Skrutskie M. F., Cutri R. M., Stiening R., et al. 2006, AJ 131, 1163

Sevenster, M. N., Prasenjit, S., Valls-Gabaud, D., & Fux, R. 1999, MNRAS, 307, 584

Stanek, K. Z., Udalski, A., Szymanski, M., Kaluzny, J., Kubiak, M., Mateo, M., & Krzeminski, W. 1997, ApJ 477, 163

Steinmetz, M., Zwitter, T., Siebert, A., et al. 2006, astro-ph/0606211

Unavane, M. & Gilmore, G. 1998, MNRAS, 295, 145

van der Kruit, P. C. 1971, A&A, 13, 405

van Loon, J., Gilmore, G. F., Omont, A. et al. 2003, MNRAS, 338, 857

Weinberg, M. D. 1992, ApJ, 384, 81

Zhao, H. 2000, MNRAS, 316, 418

A. Difference in maximum density along the line of sight and the position of the major axis

The position of the maximum density along the line of sight is not coincident with the the position of the major axis of a triaxial structure unless it be very thin (a bar) rather than a thick bulge. Two effects produce the difference: i) the most important is that the line of sight reaches its maximum at the tangential point to the innermost ellipsoid and this is not in general in the major axis (see Fig. 6); ii) moreover, in off-plane regions, the lines of sight are not parallel to the plane $b = 0$—the larger the distance the farther away from the plane and the lower the densities become, so the maximum of the line of sight is indeed closer than the real maximum in a plane parallel to $b = 0$.

We can derive analytically this difference ($\Delta r = r_m - r_a$) between the maximum density position along the line of sight (r_m), and the intersection of the line of sight with the major axis (r_a) for the case of triaxial ellipsoids with density decreasing monotonically outwards. The ellipsoidal isodensity contours are defined by the points of space with the same value of t:

$$t = \sqrt{x_1^2 + (x_2/A)^2 + (x_3/B)^2}. \tag{A1}$$

A and B are the axial ratios of the second and third axes with respect to the major axes of the ellipsoids, and x_i are the cartesian coordinates with the axis of the ellipsoids centred on the Galactic Centre; that is,

$$x_1 = x \sin\alpha - y \cos\alpha, \tag{A2}$$

$$x_2 = x \cos\alpha + y \sin\alpha, \tag{A3}$$

$$x_3 = z. \tag{A4}$$

We have assumed that the minor axis is perpendicular to the Galactic plane ($x_3 = z$). x, y, z are the cartesian coordinates with XY defining the plane of the Galaxy, centred on the Galactic Centre, with the y-axis in the Sun–Galactic Centre line. α is the angle between the major axis of the ellipsoid and this y-axis. That is,

$$x = r \sin l \cos b, \tag{A5}$$

$$y = r \cos l \cos b - R_\odot, , \tag{A6}$$

$$z = r \sin b. \tag{A7}$$

The maximum density, the tangential point of the line of sight with the innermost ellipsoid, i.e. maximum density, follows

$$\frac{\partial t}{\partial r}(r_m) = 0. \tag{A8}$$

Equation (A8) with (A1) lead together to

$$x_1(r_m)\frac{\partial x_1}{\partial r}(r_m) + \frac{x_2(r_m)}{A^2}\frac{\partial x_2}{\partial r}(r_m) + \frac{x_3(r_m)}{B^2}\frac{\partial x_3}{\partial r}(r_m) = 0, \tag{A9}$$

which with all the above expressions lead to

$$r_m = \frac{\frac{R_\odot}{\cos b}\left[\cos\alpha + \frac{\tan(l+\alpha)\sin\alpha}{A^2}\right]}{\cos(l+\alpha) + \frac{1}{A^2}\sin(l+\alpha)\tan(l+\alpha) + \left(\frac{\tan b}{B}\right)^2 \frac{1}{\cos(l+\alpha)}}, \tag{A10}$$

while the position of the major axis (simple geometry with the application of the sine rule, see Fig. 6) is

$$r_a = \frac{R_\odot}{\cos b}\frac{\sin\alpha}{\sin(l+\alpha)}. \tag{A11}$$

Both expressions for r_m and r_a are coincident for $A \ll$ (very elongated ellipsoids) and $\tan b \ll$ (in the plane), but the remaining cases are affected by a non-negligible systematic error, Δr. Calculations are carried out for $A = 0.11$, $B = 0.04$, $\alpha = 43°$, typical of a long bar: Fig. 7. The low thickness of the bar (around 1 kpc thick) is justifiable because of the low dispersion of the red clump giants (see section 4). The result is that Δr is negligible for the bar, less than $\sim$50 pc of systematic error within $|b| < 1°$. However, it is not negligible for the bulge, which reaches a discrepancy of up to 1000 pc (Cabrera-Lavers et al. 2006b).

B. Difference in maximum density along the line of sight and the maximum of star counts vs. magnitude

The maximum of star counts vs. magnitude is not strictly coincident with the maximum in density along the line of sight. The distribution of the magnitude histogram counts in a solid angle ω is indeed (assuming a constant absolute magnidude M for all red clump stars and extinction $E(r)$ along the line of sight):

$$A(m)dm = \omega r^2 \rho(r) dr, \tag{B1}$$

$$r = 10^{\frac{m-M+5-E(r)}{5}} \tag{B2}$$

Strictly speaking, we would need to transform $A(m)dm$ into $\rho(r)dr$, and then fit its maximum. From the relationship between $\rho(r)$ and $A(m)$ it can be deduced that the difference

between the corrected distance to the maximum in the density distribution (r_m^* such that $\rho'(r_m^*) = 0$) and the distance obtained to the maximum in the counts histograms (r_m such that $A'(m[r_m]) = 0$) is [neglecting the term $E'(r)$]:

$$A(m) \propto r^3 \rho(r), \tag{B3}$$

$$r_m^* = r_m + \Delta r_m \tag{B4}$$

$$\Delta r_m = \frac{3\ \rho(r_m)}{r_m \rho''(r_m)}. \tag{B5}$$

As $\rho''(r_m) < 0$, then $r_m^* < r_m$, thus the corrected distances are slightly lower than those obtained from the maximum of the magnitude histograms. This effect is more noticieable for the bulge component than for the long thin bar, as $\rho''(r_m)$ is very large for the bar. Cabrera-Lavers et al. (2006b) have estimated the range of values for Δr_m both for the bulge and for the bar, and have found the true density distributions along the line of sight. Δr_m ranges from 100 to 300 pc in bulge fields, whereas for bar fields the effect is almost negligible with corrections in the order of 25–50 pc.

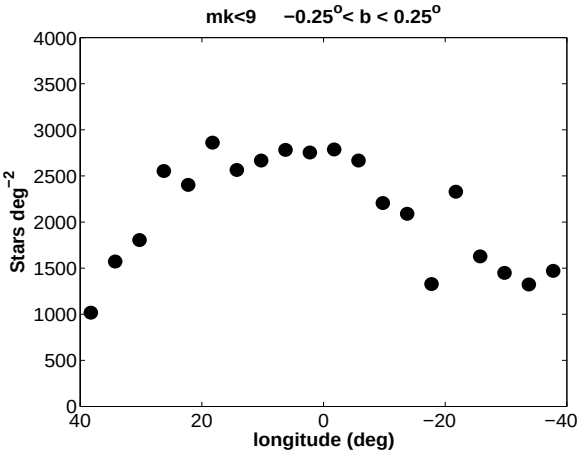

Fig. 1.— 2MASS star counts showing the asymmetry in the plane between positive and negative longitudes in $|l| < 30°$. Counts have been averaged over $\Delta l = 5°$

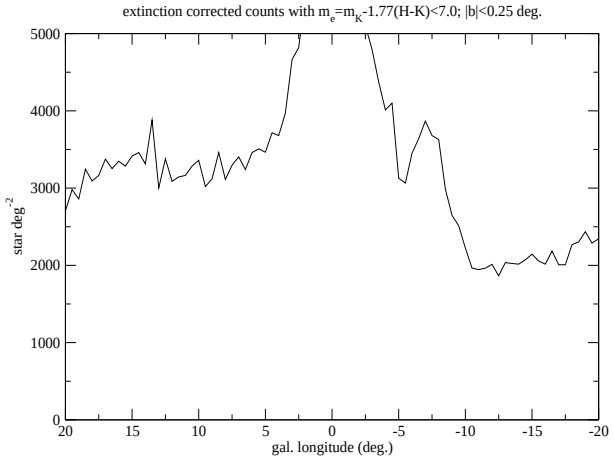

Fig. 2.— *2MASS* star counts corrected for extinction with the data used in López-Corredoira et al. (2005).

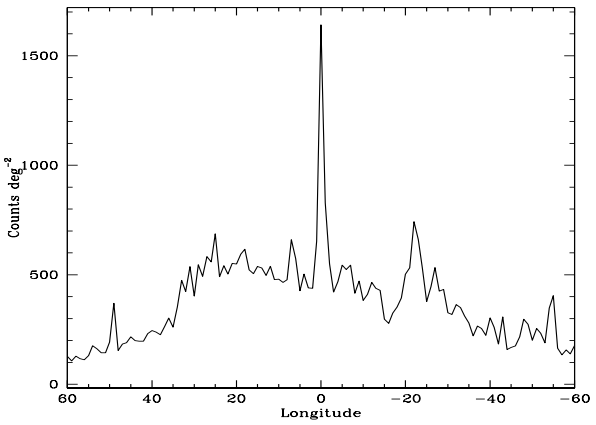

Fig. 3.— *MSX* star counts, $m_{[8.7\mu m]} < 6.0$, at $-0.5^\circ < b < 0.5^\circ$, averaged over $\Delta l = 1^\circ$, showing the asymmetry in the plane of positive and negative longitudes, and the deficit of stars at l between -15 and -18 degrees (between the hypothetical end at negative longitudes of the bar and the ring).

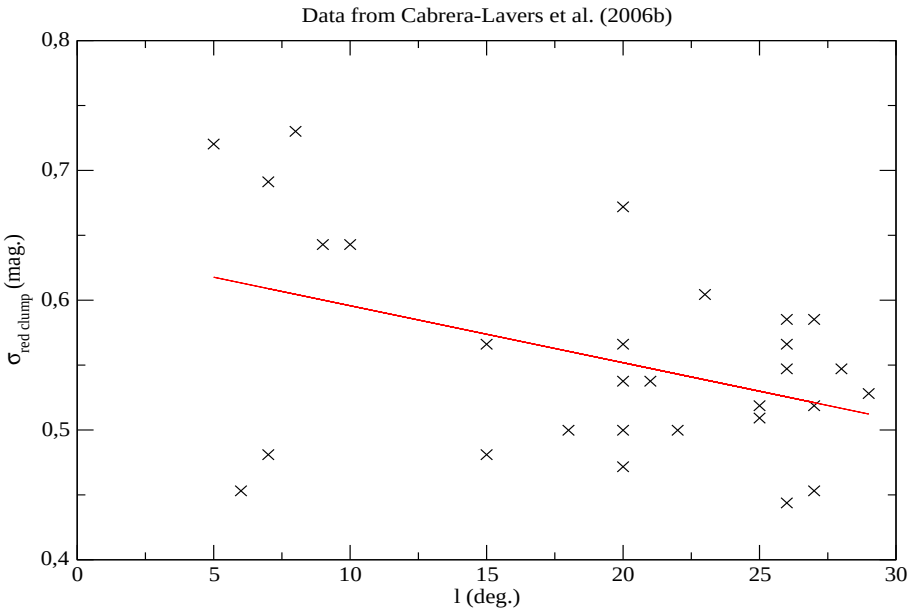

Fig. 4.— Width of the red clump (Cabrera-Lavers et al., in preparation) with $|b| \leq 1^{\circ}$. The solid line is the best linear fit: $y = 0.64 - 0.0044\ l$.

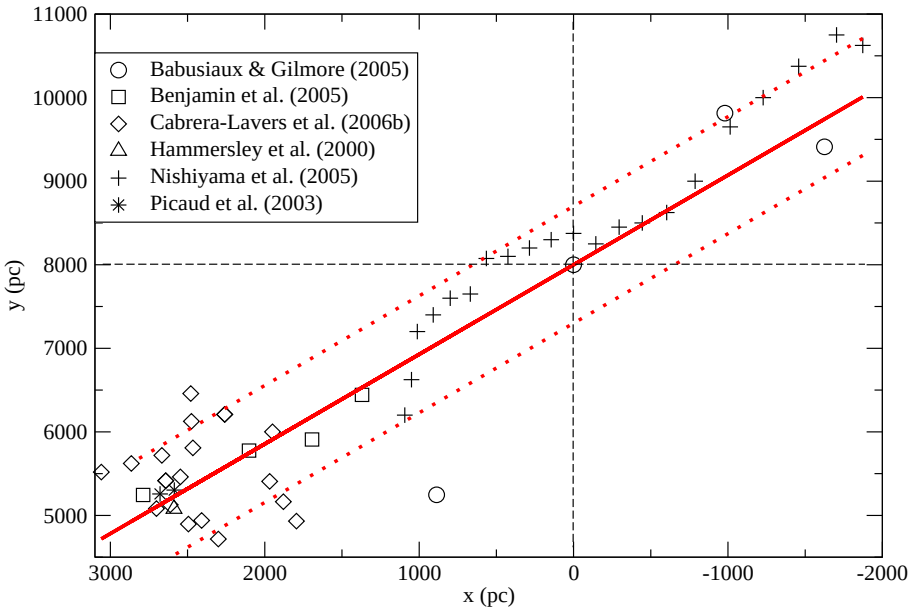

Fig. 5.— Position of the long bar with respect to the Sun according to distances derived with the red clump method. Galactic Centre at x=0, y = 8000 pc. The H00 bar with a position angle of 43° is represented by solid thick lines (and a width of 1.4 kpc is represented by dotted thick lines).

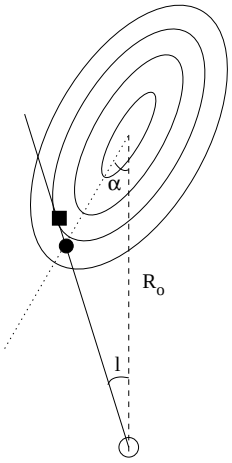

Fig. 6.— Graphical representation of the difference between the maximum density position along the line of sight (filled square) for triaxial ellipsoids and the intersection of their major axes with the line of sight (filled circle).

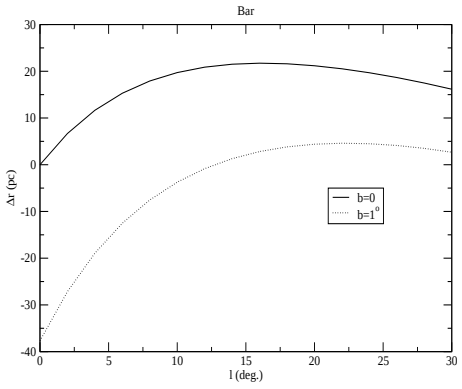

Fig. 7.— Difference between the maximum density position along the line of sight for triaxial ellipsoids of axial ratios 1:0.11:0.04, angle with the line Sun–Galactic centre 43° (expected for the long bar), and the intersection of their major axes with the line of sight.